Turk J Phys
29 (2005) , 105 – 114.

Optical Characterization of Chemical Bath Deposited Bismuth Oxyiodide (BiOI) Thin Films

F. I. EZEMA[1,2]
[1] *Department of Physics and Astronomy*
[2] *School of General Studies, Natural Sciences Unit*
University of Nigeria, Nsukka, Enugu State-NIGERIA
fiezema@yahoo.com

Received 26.10.2004

Abstract

Thin films of Bismuth oxyiodide (BiOI) were deposited, using chemical bath deposition techniques. The films were characterized using energy dispersive x-ray fluorescence (EDXRF) and Fourier transform infrared (FTIR) spectroscopy for chemical composition, and a spectrophotometer for the analysis of spectral absorbance / transmittance / reflectance.

Deposited film thickness ranged between 0.115 and 0.140 μm. The optical properties deduced from the spectral absorbance / transmittance / reflectance include the maximum values of the refractive index n that ranged between 2.62 and 2.64, the extinction coefficient k ranged between 25.84 $\times$ 10^{-3} and 42.92 $\times$ 10^{-3} while the Optical conductivity σ ranged between 0.60 $\times$ 10^{14} S^{-1} and 0.75 $\times$ 10^{14} S^{-1}.

The spectral analysis revealed that some of the films grown are poor transmitters of UV but have good transmission in the VIS-NIR regions. Some of the films show transmittance above 78% in the VIS-NIR regions and a wide band gap that ranged between 3.20 and 3.40 eV. In the mid infrared regions transmittance ranged between 3 and 37%. These properties make the film potential material for poultry protection and warming coatings, solar control and antireflection coatings and as well material for solar cell fabrication.

Key Words: Chemical bath deposition technique; Bismuth oxy iodide; poultry protection and warming coating; solar control and antireflection coatings and solar cells.

1. Introduction

The process of thin film deposition involves the deposition of material atom-by-atom, molecule-by-molecule, ion-by-ion or cluster-of-species-by-cluster-of-species condensation [1]. This methodology is applied extensively in the manufacture of photocells and is being used in optical coating, microelectronics, surface science engineering and other technologies [2]. The technique of chemically depositing thin films has the advantage of being a low cost and applicable to the production of large-area devices [3–4]. Various aspects of chemically deposited thin films have been reported [2, 4–24]. The effect of solar radiation and ultrasonification on the various properties of thin films has been reported [2, 8]. Moreover, the effect of varying growth parameters, such as deposition rate, bath composition and bath temperature, on the various properties of thin films have also been reported by several workers [3, 15–17, 25–32]. This paper reports the chemical bath deposition of BiOI thin films that would be adequate for solar and industrial applications, and are characterized using optical methods. Optical studies using transmittance and reflectance data from samples prepared using chemical bath deposition have been reported [11, 18–24].

2. Experimental Detail

Depositions of bismuth oxyiodide (BiOI) [33] films were based on the reaction between triethanolamine (TEA) complex of bismuth and potassium iodide in cold water. The film growth reaction baths were composed from quantities of $Bi(NO_3)_3{\cdot}5H_2O$, TEA and KI solutions combined successively into 50 ml beakers. The mixtures were stirred thoroughly using a glass rod at each stage to obtain homogenously mixed solutions. Each bath was made of up-to 40 ml with distilled water and allowed to stay for 24 hours dip times. The deposition of the film followed the process reported earlier on BiClO [23] and was achieved via the chemical reactions involving TEA as illustrated in the following reaction steps:

$$\begin{aligned}
Bi(NO_3)_3{\cdot}\, 5H_2O + TEA &\rightleftharpoons [Bi(TEA)]^+ + 3NO_3^- \\
Bi[TEA]^+ &\rightleftharpoons Bi^+ + TEA \\
3KI + H_2O &\rightleftharpoons 3K^+ + 3I^- + 2OH^- \\
Bi^+ + 3I^- + 2OH^- &\rightleftharpoons BiOI\downarrow + H_2O
\end{aligned}$$

The variation of the bath composition and concentration is shown in table.

Table. Variation of bath composition and concentration.

Reaction bath	$Bi(NO_3)_3{\cdot}5H_2O$		Triethanolamine		Potassium iodide		Water	
	Concentration (M)	Volume (ml)	Concentration (M)	Volume (ml)	Concentration (M)	Volume (ml)	Volume (ml)	pH
BI3	0.1	10.0	1.2	10.0	1.0	6.0	14	8.4
BI7	0.1	10.0	1.2	4.0	1.0	10.0	16	7.9
BI9	0.1	10.0	1.2	8.0	1.0	10.0	12	8.2

BiOI films were deposited on 26 mm × 76 mm × 1 mm commercial microscopic glass slides at initial bath solution pH of 8.0 to 10.0. The glass slides were previously degreased in nitric and hydrochloric acids for 48 hours, cleaned with detergent, rinsed with distilled water and drip dried in air. The substrates (glass slides) were then inserted and suspended vertically from synthetic foam, which cover the beakers containing the solutions. After 24 hours dip times, the substrates were withdrawn, rinsed and drip-dried in air. The films were characterized for the absorbance, transmittance and reflectance characteristics using a Pye-Unicam SP8-100 UV-VIS-NIR spectrophotometer. Energy dispersive x-ray fluorescence (EDXRF) was used to determine the composition of the films while the use of single-beam Fourier transform spectroscopy involve dissolving the films in nujol to determine the peaks in the far infrared regions.

3. Theoretical Consideration and Calculations

In both crystalline and amorphous semiconductors, the absorption coefficient near the fundamental absorption edge is dependent on the photon energy. In the high absorption region, the absorption coefficient takes on the following more general form as a function of photon energy [34–35]. For direct transitions,

$$\alpha h\nu = A(\alpha h\nu - E_g)^n \tag{1}$$

and for indirect transitions

$$\alpha h\nu = B(\alpha h\nu - E_g)^n, \tag{2}$$

where ν is the frequency of the incident photon, h is Planck's constant, A and B are constants, E_g is the optical energy gap and n is the number which characterizes the optical processes. n has the value $1/2$ for the direct allowed transition, 3/2 for a forbidden direct allowed transition and 2 for the indirect allowed transition. When the straight portion of the graph of $(\alpha h\nu)^n$ against $h\nu$ is extrapolated to $\alpha = 0$ the intercept gives the transition band gaps.

For semiconductors and insulators (where $k^2 << n^2$) there exists a relationship between R and n given by [11, 36]

$$R = (n-1)^2/(n+1)^2. \tag{3}$$

There is also a relationship between k and α given by [35]

$$K = \alpha\lambda/4\pi, \tag{4}$$

where α is the absorption coefficient of the film and λ is the wavelength of electromagnetic wave. The relationship between ε and k is given by [35]

$$\varepsilon = \varepsilon_r + \varepsilon_I = (n + ik)^2, \tag{5}$$

where ε_r and ε_i are the real and imaginary parts of ε, respectively.

Optical conductivity σ_o is given by [35]

$$\sigma_o = \alpha nc/4\pi \tag{6}$$

where c is the velocity of light.

Optical method as discussed by Theye [37] and Ezema [38] was used to estimate the thickness of the film.

4. Results and Discussion

Under EDXRF, the bismuth peak appeared at 10.83 keV while the iodide peak appeared at 3.93 keV.

The blank background of infrared spectroscopy for nujol and nujol mull of BiOI are shown in Figure 1. Nitrogen from bismuth nitrate was not introduced into the film, as reported for its compounds [39]. NO_2^- has absorption bands 1385–1323 cm^{-1}, 1262–1231 cm^{-1} and 862–815 cm^{-1}, while NO_3^- has absorption bands 1400–1354 cm^{-1} and 869–808 cm^{-1}. Szafran et al. [40] reported peaks between 690 and 400 cm^{-1} are due to bonds formed from the heavier species OI; hence, the peaks observed at 540 cm^{-1}are attributed to the OI species. According to Conley (39), Characteristic absorption bands of IO_3^- occur between 723 and 785 cm^{-1}, but were not observed in the film. The infrared spectroscopy of a blank background for nujol indicates peaks at 1377 cm^{-1}, 1461 cm^{-1}, 2855 cm^{-1}, 2924 cm^{-1}, 2953 cm^{-1} and 3436 cm^{-1} with transmittance between 5–57%. When the film was dissolved in nujol, the solution exhibited peaks at 1033 cm^{-1}, 877 cm^{-1}, 713 cm^{-1} and 540 cm^{-1} with transmittance between 61–68%. However the new nujol peaks show transmittance ranged between 42 and 60%. The transmittance of the film with regard to nujol peaks before dissolving the film and to new nujol peaks after dissolving the film shows that percentage transmittance ranged between 3 and 37%. That is, transmittance through solution bearing the dissolution of the film is observed to be less than transmittance through blank nujol. This means that the film suppresses transmittance within the far infrared regions.

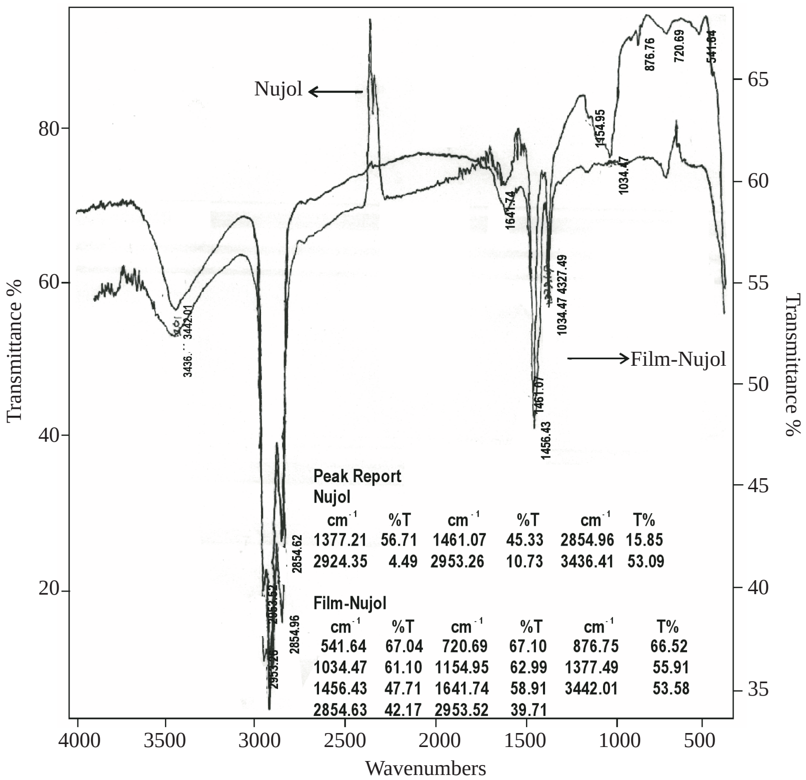

Figure 1. Spectral infrared transmittance of platin nujol/combined film-nujol system for BiOI sample.

The spectral absorbance of the films is shown in Figure 2. In the UV regions, film produced via reaction bath BI3 absorbs heavily, but at 340 nm the absorbance decreases from 0.688 to a minimum of 0.080 at 440 nm in the VIS region, from where the absorbance increases with wavelength to a maximum of 0.112 at 700 nm, and then decreased to a minimum of 0.111 in the NIR region. In the UV regions, the absorbance of films produced in BI7 reaches a maximum of 0.622 at 300 nm, decreases with wavelength to 0.074 at 400 nm, which is at the onset of the VIS region. The absorbance at VIS-NIR regions ranges between 0.059 and 0.080 with minimum in the NIR regions but maximum at the VIS regions of 600 nm. BI9 absorbs heavily in the UV regions, but at 360 nm the absorbance decreases from 0.651 to a minimum of 0.095 at 560 nm in the VIS regions from where the absorbance increases with wavelength to 0.127 at 700 nm and then decreased to a minimum of 0.111 at the NIR regions.

The spectral transmittance-reflectance of the films are shown in Figure 3. The transmittance of BI3 increases from 21% at 340 nm in the UV region to 84% at 460 nm in the VIS region, but decreases with wavelength to 78% at 800 nm. The transmittance in the VIS-NIR regions ranges between 78 and 84%, while reflectance ranges between 8 and 14%. The transmittance of BI7 increases from 24% at 340 nm in the UV region to 84% at 400 nm; and from the onset of the VIS region transmittance ranged between 84% and 87%, with reflectance ranging between 7–8% throughout the VIS-NIR regions. The reflectance in the UV region ranges between 8–20%. That there is heavy absorbance in the UV region and high transmittance in the VIS-NIR regions makes BI3 and BI9 good materials for the construction of poultry roofs and walls and for coating eyeglasses. BI7 for its spectral characteristics show good material as antireflection and thermal control coatings.

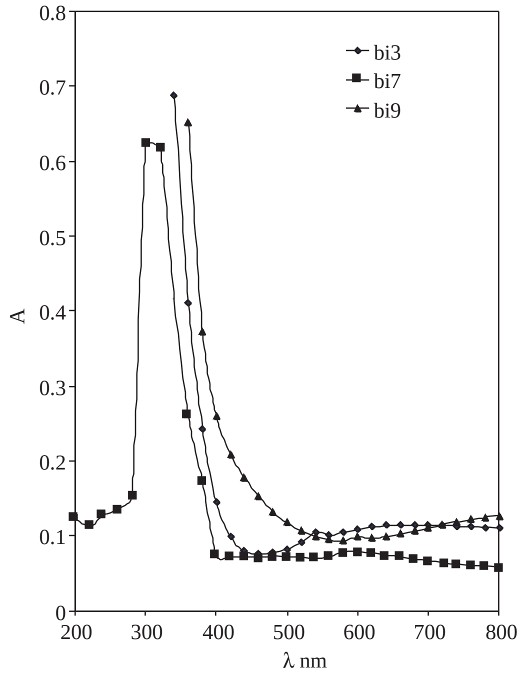

Figure 2. Absorbance (A) as a function of wavelength (λ) for BiOI thin film at 300 K.

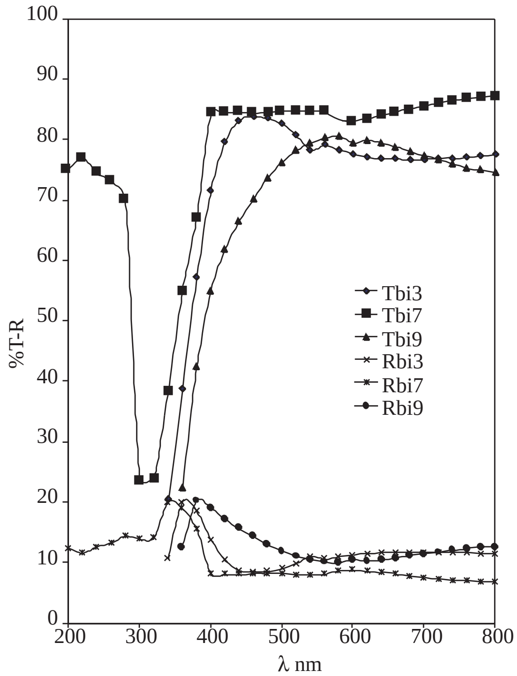

Figure 3. Transmittance (T) and reflectance (R) as function of wavelength (λ) for BiOI thin film at 300 K.

The plots of α against $h\nu$ are shown in Figure 4. These show sharp absorption edges, which are characteristics of the crystalline state of the film. The region $\alpha > 10^4$ cm^{-1} corresponds to a transition between extended states in both valence and conduction bands, while in the region $\alpha \leq 10^4$ cm^{-1} absorption exhibits rough exponential behavior [41].

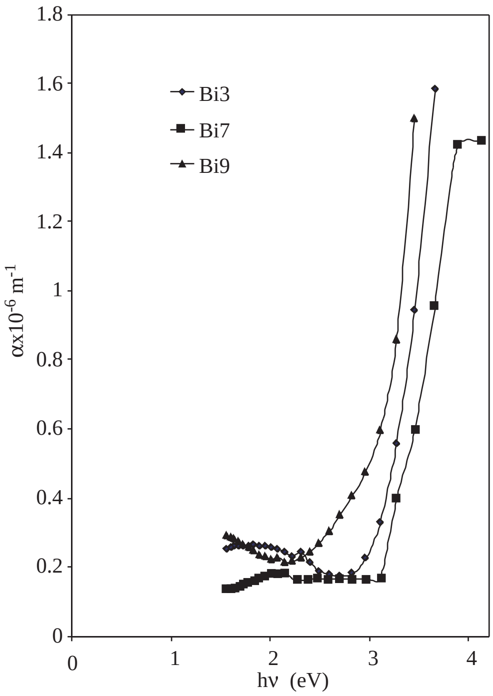

Figure 4. Plots of as function of ploton energy (hν) for BiOI thin film at 300 K.

The plots for location of the direct and indirect transition band gaps are shown Figures 5 and 6. The direct band gap values range between 3.20 and 3.40 eV, while the indirect band gap is located around 2.80 eV. BI7 exhibited high transmittance, greater than 80%, within the VIS region and has a wide band gap of 3.40 eV, a requirement for a transparent conducting oxide. Hence BI7 may be a good material for the window layer on solar cells.

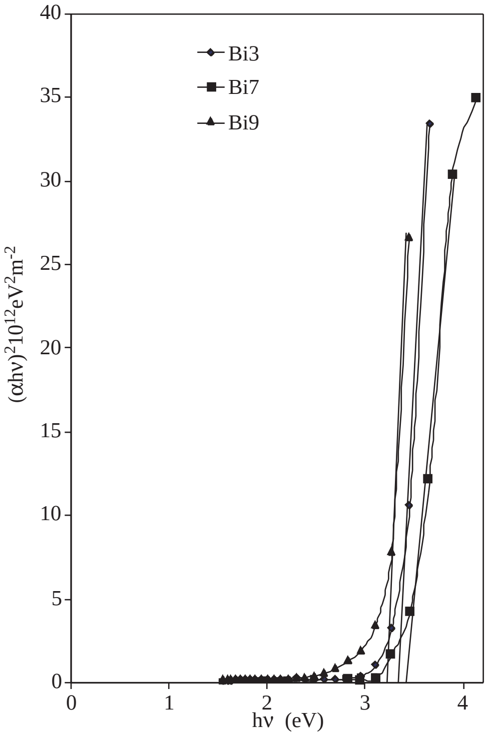

Figure 5. Plots of $(\alpha h\nu)^2$ as a function of photon energy ($h\nu$) for BiOI thin film at 300 K.

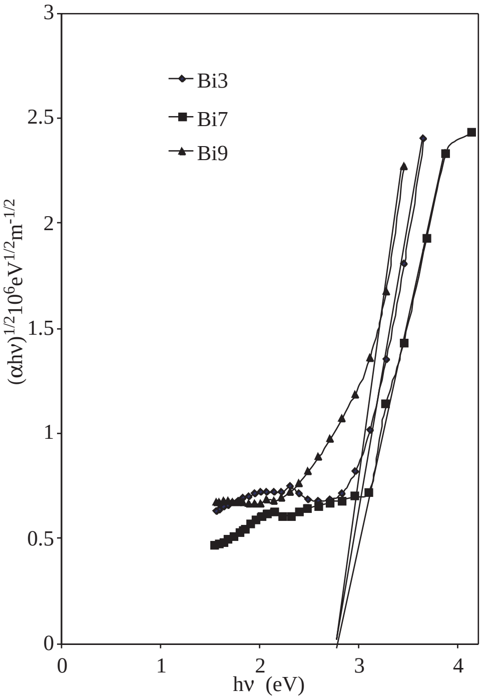

Figure 6. Plots of $(\alpha h\nu)^{1/2}$ as a function of photon energy ($h\nu$) for BiOI thin film at 300 K.

Plots of n and k against $h\nu$ are displayed in Figures 7 and 8. Peak values for n range between 2.62 and 2.64 with minimum values for n ranging between 1.71 and 1.93. Maximum k values range between 2.584×10^{-2} and 4.294×10^{-2} with minimum values ranging between 5.38×10^{-3} and 9.74×10^{-3}.

Plots of ε_r and ε_i against $h\nu$ are displayed in Figures 9 and 10. Peak values for ε_r range between 6.87 and 6.98 with minimum values ranging between 2.70 and 3.71. Maximum ε_i values range between 5.757×10^{-2} and 16.893×10^{-2} with minimum values ranging between 19.46×10^{-3} and 37.71×10^{-3}.

The plots of σ_o against $h\nu$ are displayed in Figure 11. Maximum values for σ_o range between 0.60×10^{14} S^{-1} and 0.75×10^{14} S^{-1} with minimum values ranging between 0.055×10^{14} S^{-1} and 0.099×10^{14} S^{-1}.

Figure 12(a–c) shows optical micrographs of BiOI thin film deposited at different pH values. The optical micrographs (magnification 100×) of the as-deposited films at different pH reveal good film uniformity over significant surface area of a continuous and a particulate phase. Variations in the morphology of the film show that the variations of the pH of the deposition baths affect the structure of the film and as well the absorption coefficient.

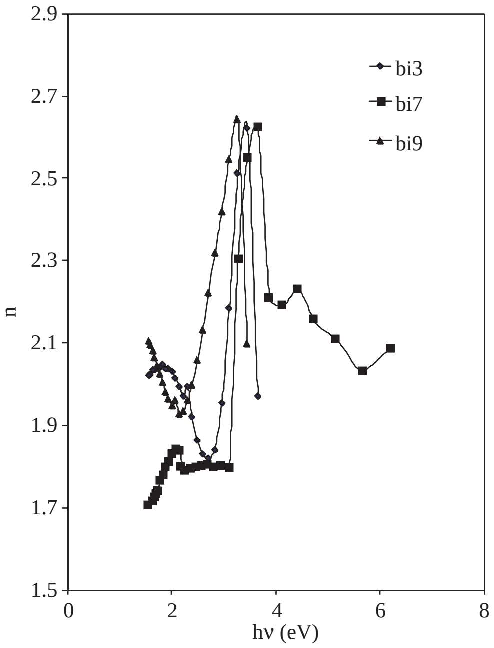

Figure 7. Refractive index (n) as function of photon energy (hν) for BiOI thin film at 300 K.

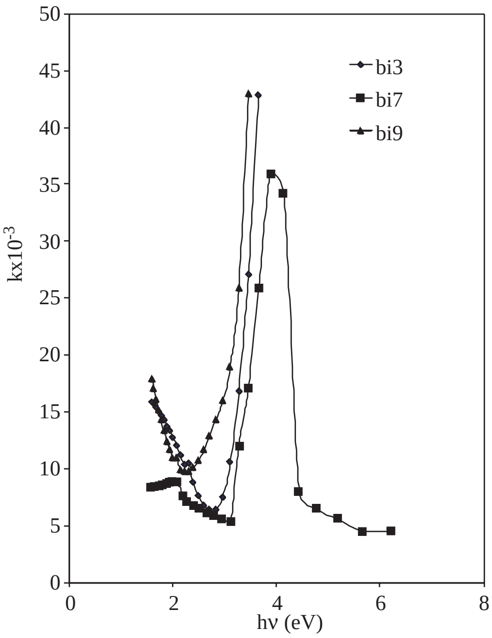

Figure 8. Extinction (k) as function of photon energy (hν) for BiOI thin film at 300 K.

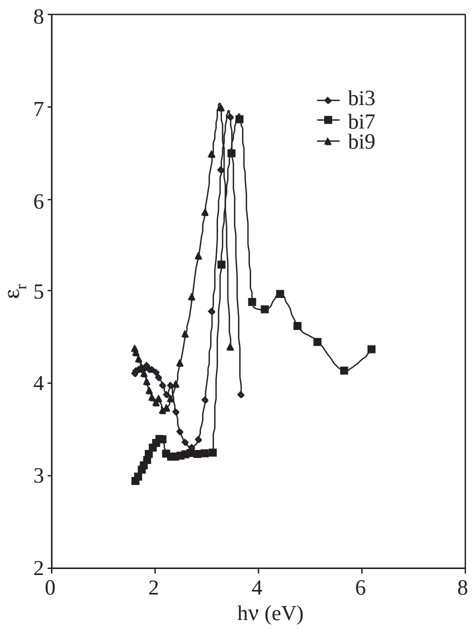

Figure 9. Real dielectric constant (ε_r) as function of photon energy (hν) for BiOI thin film at 300 K.

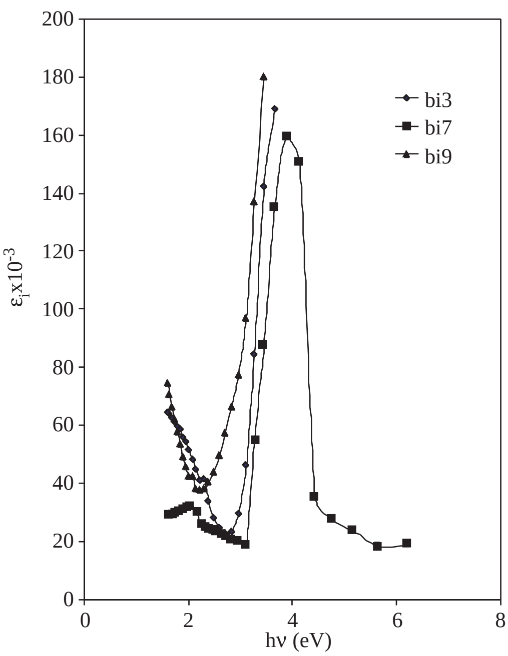

Figure 10. Imaginary Dielectric (ε_i) as function of photon energy (hν) for BiOI thin film at 300 K.

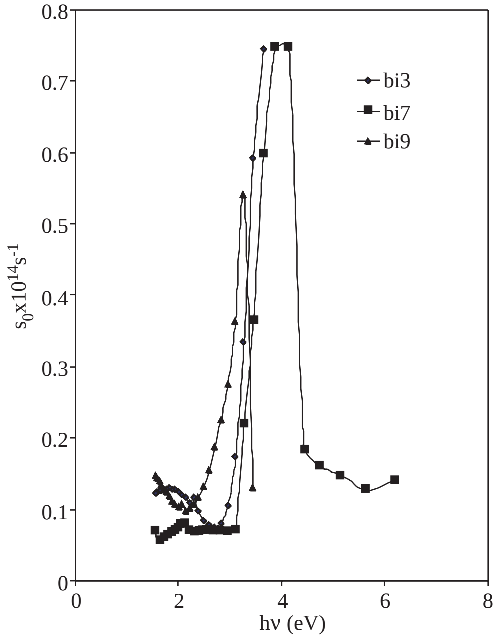

Figure 11. Optical Conductivity (σ_o) as function of photon energy (hν) for BiOI thin film at 300 K.

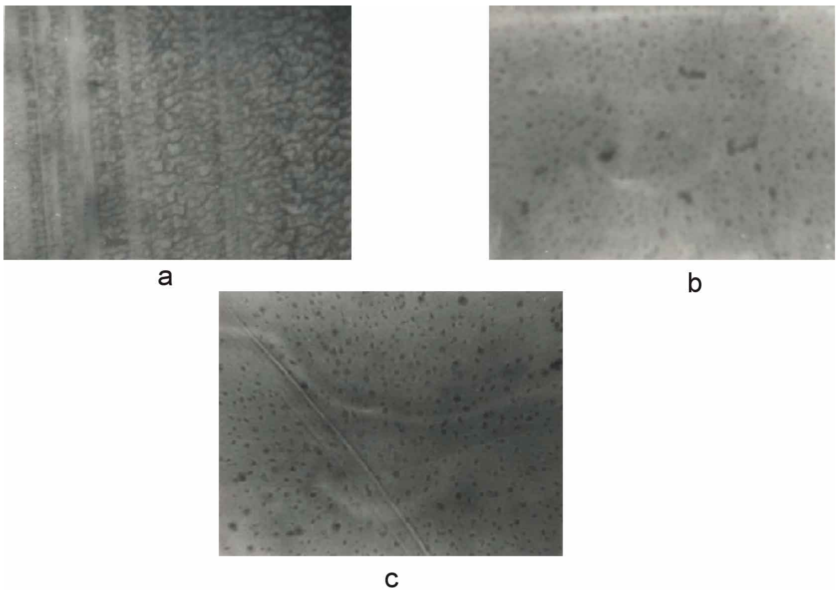

Figure 12. a-c: Optical micrograph (magnification $\times$ 100) of BiOI thin film.

5. Conclusion

Thin films of Bismuth oxy iodide (BiOI) were deposited, using chemical bath deposition techniques. The films were characterized using energy dispersive x-ray fluorescence (EDXRF) and Fourier transform infrared (FTIR) spectroscopy and spectrophotometer.

Thickness of the films deposited ranged between 0.115 and 0.140 μm. The optical properties deduced include the peak values of the refractive index n that ranged between 2.62 and 2.64, the extinction coefficient k that ranged between 25.84 $\times$ 10^{-3} and 42.92 $\times$ 10^{-3}, while the optical conductivity σ ranged between 0.60 $\times$ 10^{14}S^{-1} and 0.75 $\times$ 10^{14} S^{-1}.

The spectral analysis revealed that some of the films grown are poor transmitters of UV but exhibit very good transmission in the VIS-NIR regions. The transmittances show between 78 and 87% in the VIS-NIR regions while in the far infrared regions transmittance ranged between 3 and 37%. The films have potential applications for poultry protection and warming coatings, solar control and antireflection coatings and as well as solar cell absorbers.

References

[1] K. L. Chopra, and S. R. Das, Thin Solar Cells, (Plenum Press New York), (1983).R.

[2] Roseberg, T. S. Kuan and H. J. Hovel, *Physics Today*, **33**(5), (May 1980), 41. J.Y.

[3] K. J. Choi, J. B. Kim, Yoo and D. Kim, *Sol. Ener.*, **64**(1–3), (1998), 41.

[4] P. K. Nair, M. T. S. Nair, A. Fernandez and M. Ocampo, *J. Phys. D. Appl. Phys.*, **22**, (1989), 829.

[5] P. K. Nair and M. T. S. Nair, *Semicond. Sci. Technol.*, **4**, (1989), 807.

[6] P. K. Nair and M. T. S. Nair, *Semicond. Sci. Technol.*, **7**, (1992), 239.

[7] P. K. Nair, M. Ocampo, A. Fernandez and M.T.S. Nair, *Sol. Ener. Mater.*, **20**, (1990), 235.

[8] P. K. Nair and M. T. S. Nair, *Sol. Ener. Mater.*, **15**, (1987), 431.

[9] M. T. S. Nair and P. K. Nair, *Semicond. Sci. Technol.*, **4**, (1989), 191.

[10] P. K. Nair and M. T. S. Nair, *Solar Cells*, **22**, (1987), 102.

[11] I. C. Ndukwe, *Sol. Ener. Mater. Sol. Cells*, **40**, (1996), 123.

[12] R. Ortega-Borges, and D. Lincot, *J. Electrochem. Soc.,* **140**, (1993), 3464.

[13] G. K. Padam, and S. U. M. Rao, *Sol. Ener. Mater.,* **13**, (1986), 297.

[14] P. S.Pramanik, R. N. Bhattacharya and P. K. Basu, *Thin Solid Films*, **149**, (1987), 181.

[15] P. J. Sabestian and H. Hu, *Adv. Mater. Opt. Electron.*, **4**, (1994), 407.

[16] K. L Chopra, R. C. Kainthla, D. K. Pandya and A. D. Thakoor, Physics of Thin Films, Vol. 12, (Academic Press New York), (1982).

[17] I. Kaur, D.K. Pandya and K.L. Chopra, *J. Electrochem. Soc.*, **127**, (1980), 943.

[18] F. I. Ezema and C. E Okeke., *Nig. Journ. Phys.*, **14**(2), (2002), 48.

[19] F. I. Ezema and C. E. Okeke, *Nig. Journ. Solar Ener.*, **14**, (2003), 68.

[20] F. I. Ezema and C. E. Okeke, *Academic Open Internet Journal,* http://www.acadjournal.com/2003/v9/part2/p4/CHEMICAL_BATH_DEPOSITION.PDF

[21] F. I. Ezema and C. E Okeke, *Greenwich Journal of Science and Technology*, **3**(2), (2003), 90.

[22] F. I. Ezema and P. U. Asogwa, *Pacific Journal of Science and Technology*, **5**(1), (2004), 33.

[23] F. I. Ezema, *Journal of the University of Chemical Technology and Metallurgy*, **39**(2), (2004), 225.

[24] F. I. Ezema., *Academic Open Internet Journal*, http://www.acadjournal.com/2004/v11/part2/p1/index.htm

[25] V. S. Karande, S. H. Mane, V. B. Pujari and L. P. Deshmukh, *Turk. J. Phys*, **27,** (2003), 559.

[26] D. S. Sutrave, G. S. Shahane, V. B. Patil and L. P. Deshmukh, *Turk. J. Phys,* **24,** (2000), 63.

[27] V. B. Pujari, V. B. Gaikwad, E. U. Masumdar,P. D. More and L.P. Deshmukh, *Turk. J. Phys*, **26**, (2002), 407.

[28] V. Estrella, M. T. S. Nair and P. K. Nair, *Semicond. Sci. Technol.*, **18**, (2003), 190.

[29] A. Nunez Rodriguez, M. T. S. Nair and P. K. Nair, *Mat. Res. Symp. Proc.*, **730,** (2002), V5.14.1.

[30] Y. Rodriguez-Lazcano, L. Guerrero, O. Gomez Daza, M.T.S. Nair and P. K. Nair, *Superficies y Vacio*, **9**, (1999), 100.

[31] Y. Rodriguez-Lazcano, M. T. S. Nair and P. K. Nair, *J. Crystal Growth,* **23**(3), (2001), 399.

[32] P. K. Nair, L. Huang, M. T. S. Nair, H. Hu, E. A. Meyers and R. A. Zingaro *J. Mater. Res.,* **12**(3), (1997), 651.

[33] N. A.Lange, Lange's Handbook of Chemistry, 14^{th} edn, (McGraw-Hill Book Co.,New York), (1992).

[34] I. M. Tsidilkovsk, Band structure of semiconductors, Pergamon Press, Oxford (1982).

[35] J. I. Pankove, Optical processes in semiconductors, Prentice-Hall, New York (1971).

[36] Janai, M., D. D. Alfred, D. C. Booth and B.O. Seraphin, *Sol. Ener. Mater.* **1**, (1979), 11.

[37] M. Theye, Optical Properties of Thin Films, (Edited by K.L. Chopra and L.K. Malhota), thin film technology and Applications, (Tata McGraw-Hill, New Delhi), (1985).

[38] F. I. Ezema, *Journal of university of science and Technology*, **23**(2), (2003), 32.

[39] R. T. Conley, Infrared spectroscopy, (Allyn and bacon Inc, Boston), (1966).

[40] Z. N. Szafran, R. M. Pike, and M. M. Sigh, Microscale inorganic Chemistry, A

[41] Comprehensive Laboratory Experience, (John Wiley and Sons Inc. New York), (1991).

[42] M. F. Kotkata, H. T. El-Shair, M. A. Afifi and M. M. A. Azizi, J. *Phys. D: Appl. Phys.***27**, (1994), 623.